Experiment and analysis of a self-centering precast reinforced concrete shear wall

A.Q. Gu & Y. Zhou

State Key Laboratory of Disaster Reduction in Civil Engineering, Tongji University, China

2017 NZSEE Conference

ABSTRACT: Earthquake resilient structure is a new trend of structures with an advantage of high resilience under earthquakes. The self-centering reinforced concrete (RC) shear wall is one kind of earthquake resilient structures. The self-centering ability of the shear wall is realized by pre-stressing the unbonded tendon in the wall. Meanwhile, with the advantages of environment friendly and short construction period, the precast structure is drawn increasing attentions. This paper proposed the concept of precast self-centering shear walls. Then cycle loading tests were carried out to study the seismic behavior of a precast RC shear wall and a precast self-centering RC shear wall. Finite element models of two shear walls are performed in ABAQUS and verified by comparison with the cycle loading test. The results indicate that the precast self-centering shear wall has better ductility and energy-dissipating ability but lower lateral resistance under the cycle loading. Compared with precast RC shear wall, it is also shown that the precast self-centering shear wall has smaller residual displacement and less damage after the cycle loading.

1 INTRODUCTION

Reinforced concrete shear wall is a common and cost effective way of providing lateral force resistance to buildings in seismic areas of the world. Historically, cast-in-place reinforced concrete has been the most commonly used method of construction for structural wall systems. More recently, there has been an increasing use of precast reinforced concrete walls. And conventional precast RC shear wall is designed to behave like cast-in-place shear walls. Under earthquakes, significant structural damage and large residual lateral displacements are expected to occur with such systems (Wood *et al.* 1987). And large lateral drifts structures were found difficult to repair after earthquakes, this would inevitably lead to expensive repair cost and business downtime (Eguchi *et al.* 1998). Hence, the cost of consequences of damage after an earthquake may be significant to the building owners.

To reduce some of the adverse effects observed with traditional concrete structural systems, Priestley and Tao (Priestley and Tao 1993) first proposed the idea of utilizing unbonded prestressed tendons in precast RC frame structures to provide the primary lateral force resistance and restoring force. The behaviour of such a system can be described as being non-linear elastic. Priestley and MacRae (Priestley and MacRae 1996) also studied the frame joints with unbonded tendons under quasi-static reversed cyclic loading tests, the test results showed that prestressed tendons can provide self-centering characteristic to structures. Kurama *et al*. (Kurama *et al.* 1996) gave the design method of precast self-centering shear walls using unbounded prestressed tendons and recommendations on selection of wall design properties such as the initial stress in tendons, amount of prestressed tendons and location of tendons. And they also conducted over 200 dynamic time-history nonlinear analysis of six, six-storey high prototype walls, using a total of 15 design level and 15 survival level ground earthquake records. The main disadvantage of this purely non-linear elastic system is the lack of energy dissipation capacity. To improve the energy dissipated ability of self-centering shear walls and reduce the response to seismic excitation, low yield strength reinforcements are incorporated at the interface of the wall and its foundation. And those self-centering walls incorporated with low yield strength reinforcements are called hybrid walls. Restrope and Rahman (Restrope and Rahman 2007) researched a hybrid shear wall under quasi-static reversed cyclic loading tests. Holden *et al*. (Holden

et al. 2003) studied a hybrid shear wall with carbon fibre tendons and steel fibre concrete, and the reinforcements of the walls are reduced compared with conventional precast walls. Dang (Dang *et al.* 2014a, b) conducted cyclic loading tests on prestressed self-centering shear walls with horizontal bottom slits, the partially bottom slits are designed to increase the energy dissipation ability of self-centering walls. In these hybrid precast shear walls, cosmetic damage of concrete is restricted to the base corners of the wall about which it rocks. Special reinforcing details in these areas limit the crushing of concrete. For hybrid precast walls, the level of hysteretic damping is improved compared with purely self-centering walls, while the self-centering characteristic is still preserved.

In this paper, one conventional precast RC shear wall (SW1) and one precast self-centering RC shear wall SW3 are studied under quasi-static reversed cyclic loading tests. Simple energy dissipation devices are introduced to SW3. Test scheme and results are described in the following sections. Simulation models are established in ABAQUS and verified by comparing with the test results.

2 TEST SCHEME

2.1 Description of specimens

Two geometric identical half-scaled shear wall specimens were tested under quasi-static reversed cyclic loading. Each specimen consists of top beam, wall and foundation. The total height of the specimen is 4.2m, the length is 1.5m, and the width is 0.2m. The height of foundation is 0.7m. Each specimen has two joints. In Each specimen, the longitudinal reinforcements are spliced by GT25 and GT12 grouted sleeves manufactured by Beijing Sida Jianmao Technology Development Company，the dimensions of the grouted sleeves are shown in Figure 1. The grouted sleeves has threaded connection at one end and grouted connection at the other end.

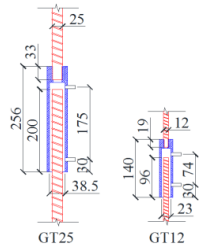

Figure 1. Dimension of grouted sleeves.

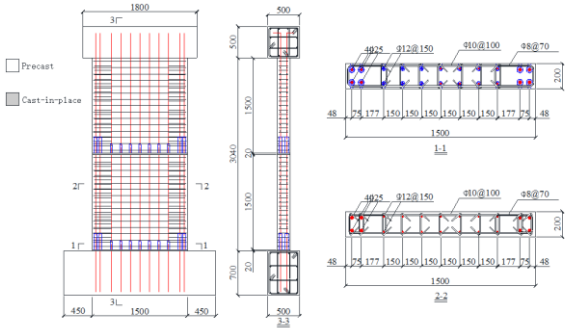

Figure 2. Reinforcement layout of SW1.

Specimen SW1 is a conventional precast shear wall designed following the Chinese Concrete Structure Design Code (GB50010-2010). SW1 is designed for ductile response using capacity design principles. Adequate detailing of the plastic hinge zone allows the structure to deform in a ductile manner, which is expected for a monolithic RC shear wall. The primary objective of SW1 is to compare the behavior of a conventional precast shear wall to that of SW3. SW1 is also used to evaluate the performance of the grouted sleeves connection which is vital for the performance of the precast shear walls. The reinforcement layout of SW1 is illustrated in Figure 2. As shown in Figure 2, HRB400Φ25 and HRB335Φ12 bars are used as longitudinal reinforcements, HPB300Φ10 bars are

used as transverse reinforcements, HPB300Φ8 bars are used as stirrups. The longitudinal and transverse distributed reinforcement ratios for this specimen are 0.75% and 0.78%, respectively. The longitudinal reinforcement ratio at the wall ends is 2.90%. The volumetric confinement reinforcement ratio is 1.87%.

Specimen SW3 is designed as a precast self-centering shear wall with simple energy dissipation devices. SW3 is designed to obtain a non-linear response, resulting in minimal damage to the specimen and achieving no residual drift. The reinforcement layout of SW3 is illustrated in Figure 3. Two steel strands are placed at 400mm from each edge of wall, respectively. And the cross section area of steel strands is 140mm^2. The initial level of prestressing in steel strands is 0.5fpu, where fpu is the strands ultimate tensile strength. The ultimate tensile strength of steel strands in this paper is 1977 MPa. Two steel plates are placed at the wall corners of each side to protect the wall base from damage. The thickness of the steel plate is 10mm, the width is 200mm, and the length is 325mm. The mechanism diagram of energy dissipation devices is shown in Figure 4. The steel sleeves encircling the longitudinal reinforcements are aimed to separate steel bars and prevent buckling of steel bars in compression. The partially unbounded longitudinal reinforcements at the wall-foundation interface are used to increase the level of hysteresis damping.

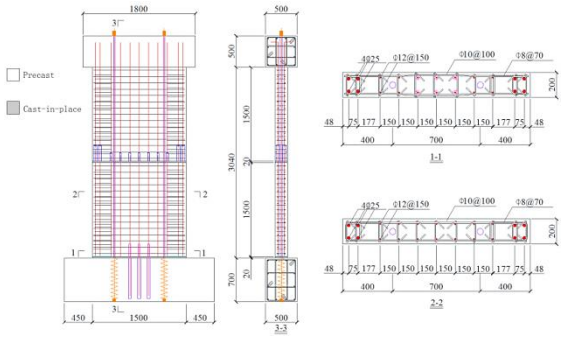

Figure 3. Reinforcement layout of SW3.

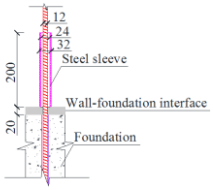

Figure 4. Mechanism diagram.

2.2 **Loading arrangement**

The restraint and loading frames used in this test are shown in Figure 5. The main reaction frame consists of a steel beam and steel columns bolted to the strong floor. Two restraint beams are arranged both side of the wall spanning the steel columns at two thirds the height of the specimen. These provide resistance to both out-of-plane deformation and twist. The foundation is secured to the strong floor through the use of four bolts at each side. These bolts provide restraint against overturning of the foundation beam once lateral force was applied to the wall.

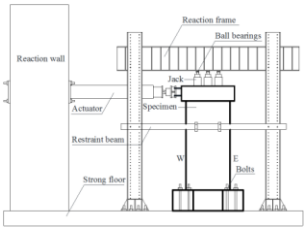

Figure 5. Schematic representation of loading arrangement.

The lateral load applied to the specimens is supplied through the use of a hydraulic actuator. This

actuator is bolted to the reaction wall at a height 4.04m from the strong floor. Gravity load is simulated via three hydraulic jacks situated top surface of each specimen. A constant axial load of 90kN is provided by the three hydraulic jacks. Ball bearings attaching the hydraulic jacks to the steel beam allow the hydraulic jacks to translate with the specimen during the tests.

2.3 **Instrumentation**

Figure 6 shows the deployment of instrumentation used to monitor displacements and deformations in each specimen. For specimen SW1, DT1 to DT5 are used to obtain average curvature of the wall panel. DT6 to DT8 are used to measure the rigid motion of the foundation. DT9 to DT12 are used to monitor the flexure and shear deformation of the specimen. DT13 to DT 18 are used to obtain the rotation of two horizontal joints. The arrangement of displacement transducer of SW3 is identical to that of SW1 except that two additional displacement transducers are applied at the wall-foundation interface in SW3. Forces in tendons are measured using two force transducers for SW3 specimen.

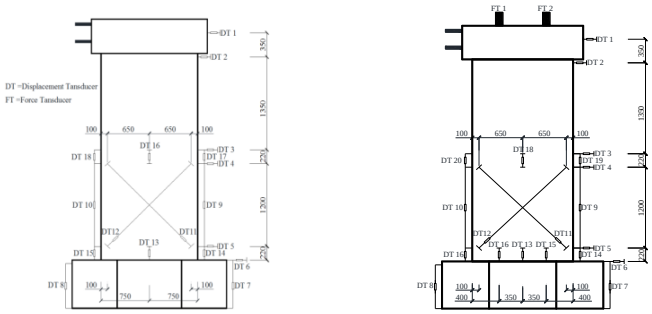

(a) SW1 (b) SW3

Figure 6. Schematic representation of the external instrumentation.

2.4 **Loading process**

Lateral loading of both specimens is quasi-static lateral displacement based cycles. The test regimes of both specimens are plotted in Figure 7. Initial cycles are within the elastic range which allowed the stiffness and yield displacement of the wall to be established. Amplitudes of initial cycles are up to ± 0.09% for SW1 and ±0.15% for SW3. Subsequent cycles compose of three-same amplitude cycles at a level. For SW1, a jump of 0.09% drift between levels is set before 1.9% drift, and a jump of 0.18% drift between levels is set after 1.9% drift. For SW3, a jump of 0.15% drift between levels is set through the test schedule. This test schedules are completed up to 2.4% for SW1 and SW3. Positive semi-cycles are those obtained by loading from East to West. Conversely, negative semi-cycles are those obtained by loading from West to East.

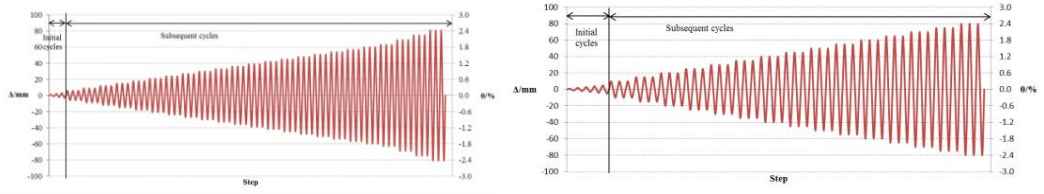

(a) SW1 (b) SW3

Figure 7. Schematic representation of the external instrumentation.

3 **OBSERVATION AND TEST RESULTS**

3.1 **Failure mode**

For specimen SW1, cracks are found at the wall base region at drift 0.63%. At drift 1.6%, the damage of SW1 is extensive, diagonal crack is observed in wall, and two longitudinal cracks develop along the upside of grouted sleeves and the wall-foundation interface, respectively. At drift 1.6%, the damage is

such that the capacity of the specimen SW1 begins to degrade. At drift 2.4%, Extensive concrete spalling at the corners of the wall and above the grouted sleeves regions result in the specimen being virtually irreparable. Hence, the failure mode of SW1 is same as that of conventional RC shear walls. For specimen SW3, a longitudinal gap along the wall-foundation interface is observed in SW3 at drift 0.6%, and SW3 begins to rock around the wall-foundation interface as expected. The prestressing strands achieve its yielding state at drift 1.05%, and the failure mode of SW3 is the yielding of steel strands. In contrast with SW1, SW3 sustains little damage in wall until drift 2.4%. Only crushing of the concrete at wall corners is observed. Figure 8 illustrates the damage to each specimen at final drift 2.4%.

(a) SW1 (b) SW3

Figure 8. Final damage states of specimens.

3.2 **Lateral force versus displacement response**

The performance of specimen SW1 shows typical characteristics of a conventional precast RC shear wall. In monolithic RC shear wall, energy is dissipated mainly through yielding of the longitudinal reinforcements at the plastic hinge region. Figure 9a illustrates the hysteretic behaviour of specimen SW1. The shape and size of the loops are not plump as that of a cast-in-place RC shear wall. The reason is that the sliding of reinforcement and grout sleeve at the threaded end affects the yielding of longitudinal reinforcements at plastic hinge region. The lateral force versus displacement response of the specimen SW3 is plotted in Figure 9b. As shown in this figure, the shape and size of the loops indicates the SW3 performs as a typical self-centering structure.

Compared the lateral force versus displacement response of two specimens, the deform ability of SW3 is better than SW1. Figure 9b shows no severe strength degradation of SW3 reach 2.4% drift, while Figure 9a shows rapidly capacity declination after SW1 reached peak lateral force.

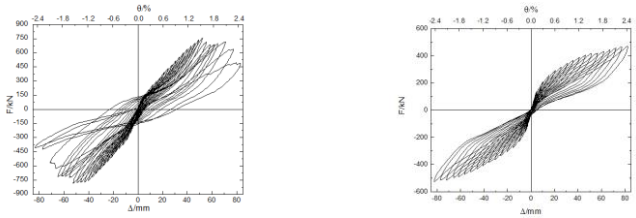

(a) SW1 (b) SW3

Figure 9. Hysteretic responses of specimens.

3.3 **Energy dissipation**

The equivalent viscous damping of first cycle at each level for SW1 and SW3 are shown in Figure 10. And Figure 11 shows the energy dissipated of the first cycle by both specimens. As Figure 10 is shown, the equivalent viscous damping of SW3 does not change considerably with the increase of lateral displacement, and the value of equivalent viscous damping is around 5% throughout the test. The equivalent viscous damping of SW1 has an increase trend with the increase of lateral displacements. And the drop off in damping of SW1 after 2% drift is due to the released energy that comes from the cracking of the concrete at the wall base. Figure 11 indicates that SW1 dissipates lager amount of energy than SW3. The decrease amount of SW1 at large drifts is because of the capacity decrease of SW1.

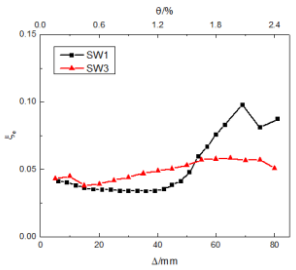

Figure 10. Equivalent viscous damping.

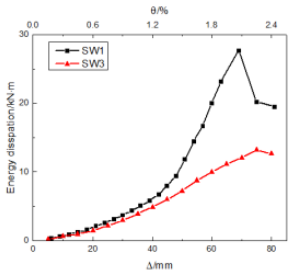

Figure 11. Dissipated energy amount.

3.4 **Residual drift**

Residual drift after a seismic event is a crucial problem associated with conventional monolithic construction. SW3 experiences a small residual drift at peak displacements well in excess 2%. The contrast of top residual drift ratios between SW1 and SW3 is shown in Figure 12. The residual drifts of SW1 are larger than that of SW3 throughout the entire test. As the lateral displacement increases, the residual drift of SW1 increases. The residual drift of SW1 reaches the maximum value of 0.9%. The residual drift of SW3 does not change vastly with the increase of lateral displacement.

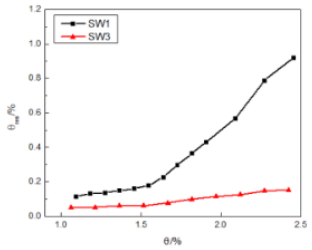

Figure 12. Comparison of the residual drifts of specimens.

4 **ANALYSIS OF SIMULATION**

Finite element models of two specimens are established in ABAQUS to simulate the backbone curves of the specimens, Figure 13 shows the selections of material constitutive models and element for the two specimens and schematic diagram of finite element model. In the finite element models, the material constitutive model of concrete elements is Concrete Damaged Plasticity Model, and that of reinforcement elements is bilinear model. The concrete elements use solid element C3D8R, and the reinforcement and steel strand elements are simulated by truss element T3D2. During the demolition of the specimens, the sliding between the longitudinal reinforcements and grouted sleeves at the threaded connection end is founded. As a result, the strength and stiffness of SW1 is weakened. Hence, the Translator is used at lateral joints to simulate the effect of sliding between reinforcements and sleeves.

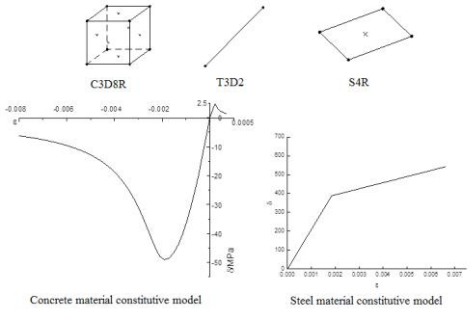

(a) material constitutive models and element selections

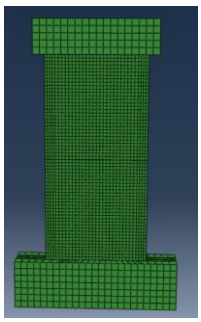

(b) Finite element model

Figure 13. Specimens modeling in ABAQUS.

Monolithic pushover analyses of two specimens are executed in ABAQUS. Figure 14 shows the comparison of the backbone curve of analysis model and test results. For SW1 specimen, the simulation is very close to the test result before the capacity decrease. Figure 14 also shows that the analytical backbone curve is close to that obtained from test, which suggests that the performance of such structures can be closely predicted.

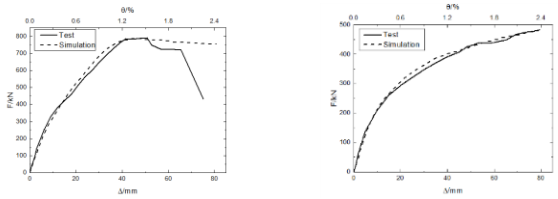

(a) SW1 (b) SW3

Figure 14. Comparison of the backbone curves of simulation and test results.

Figure 15 illustrates the MISE results of each specimen at their peak capacities. For SW1, the simulation results show that the damage is concentrated at the corners and diagonal cracks develop in specimen SW1, and the results is reasonable compared with the observation of SW1 during the test. For SW3, the modeling results indicates less damage compared with SW1, and gap opening at the wall-foundation interface is also emulated.

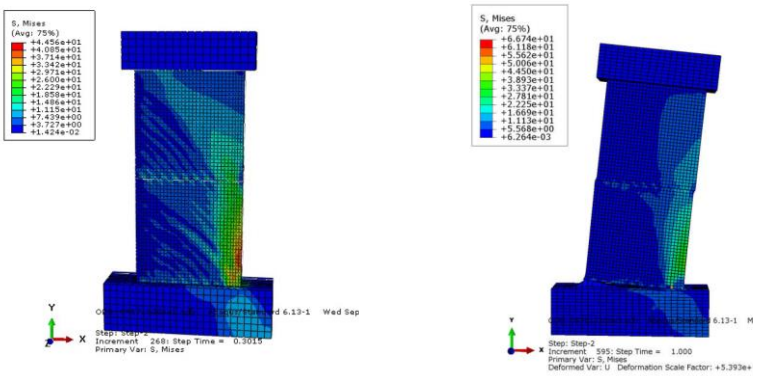

(a) SW1 (b) SW3

Figure 15. MISE results of each specimen.

5 CONCLUSIONS

Comparison is made between the test results of a precast RC cantilever wall designed to display ductile behaviour and a precast self-centering RC shear wall incorporating energy dissipation devices. Analysis models are established in ABAQUS to simulate the specimens. The results of study are summarized as follows:

1. The conventional precast RC shear wall SW1 performs as expected with energy dissipated through the formation of plastic hinge region. The specimen eventually fails due to the crack of concrete at wall toes and yielding of longitudinal reinforcements. Sliding of longitudinal reinforcement at the threaded ends of grouted sleeves is observed during the demolition of the specimen. The sliding affects the stiffness and energy dissipation ability of SW1 Specimens. Further study of the cause of sliding should be needed.
2. The precast self-centering shear wall SW3 has better deformation ability and smaller residual drift compared with SW1. And no severe strength degradation of SW3 specimen is found during the test. The energy dissipation ability of SW3 does not improve much with the incorporating of the energy dissipation devices used in this paper. Enlarging the length of unbonding steel bars and utilising low yielding point steel can be used to improve the energy dissipation ability of SW3.
3. The analysis models for both specimens give reasonable backbone curves compared with the test results.

6 ACKNOWLEDGEMENTS

This research is supported by the National Key Research and Development Program (Grant No. 2016YFC0701101) in China.

REFERENCES

Dang, X.L., Lu, X.L. & Zhou, Y. (2014a). Experimental study and numerical simulation of self-centering shear walls with horizontal bottom slit. *Journal of Earthquake Engineering and Engineering Vibration* 34(4): 154-161.

Dang, X.L., Lu, X.L. & Zhou, Y. (2014b). Experimental design and measured behavior analysis of self-centering shear walls with horizontal bottom slit. *Journal of Earthquake Engineering and Engineering Vibration* 34(6): 101-112.

Eguchi, R.T., Goltz, J.D., Taylor, C.E., Chang, S.E., Flores, P.J., Johnson, L.A. & Blais, N.C. (1998). Direct Economic Losses in the Northridge Earthquake: A Three-Year Post-Event Perspective. *Earthquake Spectra* 14(2): 245–264.

GB50010-2010. (2010). *Concrete Structure Design Code*. Beijing: China Building Industry Press.

Holden, T., Restrope J. & Mander, J.B. (2003). Seismic Performance of Precast Reinforced and Prestressed

Concrete Walls. *Journal of Structural Engineering* 129(3): 286-296.

Kurama, Y., Pessiki S., Sause, R. & Lu, Le-Wu. (1999). Seismic Behavior and Design of Unbonded Post-tensioned Precast Concrete Walls. *PCI Journal* 38(3): 72-93.

Priestly, M.J.N. & Tao, J.R.T. (1993). Seismic Response of Precast Prestressed Concrete Frames with Partially Debonded Tendons. *PCI Journal* 38(1): 58-69.

Priestly, M.J.N. & MacRae, G.A. (1996). Seismic Tests of Precast Beam-to-Column Joint Subassemblages With Unbonded Tendons. *PCI Journal* 41(1): 64-81.

Restrope, J.I. & Rahman, A. (2007). Seismic Performance of Self-Centering Structural Walls Incorporating Energy Dissipators. *Journal of Structural Engineering* 133(11): 1560-1570.

Wood, S., Wright, J. & Moehle, J. (1987). *The 1985 Chile earthquake: observations on earthquake-resistant construction in Vina del Mar*. Urbana: University of Illinois at Urbana-Champaign.